International Journal of Engineering

Preparation of Porous Alumina/Nano-Nickel Composite by Gel Casting and Carbothermic Reduction

Z. Hosseini[a,b], S. Mollazadeh Beidokhti[b], J. Vahdati Khaki[b], M. Pourabdoli*[a]

[a] Department of Materials Engineering, Hamedan University of Technology, Hamedan, Iran
[b] Department of Materials Engineering, Faculty of Engineering, Ferdowsi University of Mashhad, Mashhad, Iran

PAPER INFO	ABSTRACT
	Effects of dispersant (Tri polyphosphate sodium) amount on gel viscosity, mechanical activation of raw materials, raw materials mixture composition, and reduction atmosphere on the prepared composites and NiO reduction mechanism were investigated. It was found that 2.5 wt % dispersant is an optimum amount for a gel suspension with 50 V% of solid consisting of alumina, graphite, and nickel oxide. XRD results of reduced and sintered product (at 1200-1500 °C) showed that alumina, nickel, and nickel aluminate spinel are present in the prepared composite. The porosity of the composite made with 12 h ball milled-alumina was 48%, while it was 64 % in the sample made with 20 min ball-milled alumina. The results of TG-DTA analyses showed that the reduction temperature and mechanism are dependent on the raw materials' ball milling time. Thermal analyses revealed that mechanical activation of raw materials decreases the NiO reduction temperature and increases the metallic Ni production.

1. INTRODUCTION

From the unique advantages of hybrid composites over conventional composites are the balanced strength and stiffness, the desired mechanical properties, cost and weight reduction [1, 2]. Porous ceramic materials with a combination of metals have emerged as a new class of materials. These materials exhibit unusual mechanical and thermal properties, including energy storage, vibration and sound absorption, and thermal insulation, leading to a wide range of applications [3, 4].

Alumina-nickel bodies are attractive due to their mechanical and magnetic properties as well as their widespread use in the catalyst industry [5, 6]. The presence of porosity in the alumina body of composite increases its surface activity and uses possibility in various applications such as absorbers, filters, and electrical sensors [7]. In the preparation of alumina-nickel bodies, instead of the direct use of nickel, nickel oxide or nickel nitrate is used to supply metallic nickel

(during the reduction process) to make the uniform distribution of small nickel particles in the final body [8]. Usually, in the methods of making alumina-nickel composites, a pre-formed body of a mixture of alumina and nickel oxide is made. The body is then placed in a furnace under the flow of hydrogen gas to reduce the nickel oxide to metallic nickel. Common methods of forming alumina-nickel composites such as pressing, sol-gel, and slurry casting methods have problems that prevent their widespread use, and except for the slurry casting method, it is not possible to make a porous product with mentioned methods [7, 9-11]. The gel casting method is a relatively simple process to produce a body with final dimensions close to the original raw body. In this method, the ceramic slurry containing the polymerizable additives is poured into a mold in the desired shape. Since the particles do not have the opportunity to settle down in the slurry, they stick together due to the gelling process and take the shape of a mold. Finally, after leaving the mold, the casting part is

dried and sintered [5]. Although in the gel casting process, the slurry contains a large volume of solids (about 50% by volume or more), it still has a high fluidity [12]. The mold materials used in this method are cheap and include wax, plastic, glass, and metal [13, 14]. The amount of organic monomers in the gel casting method is very small compared to other processes, and it is easily removed during the burning of the adhesive, and the parts are strong enough to be machined [5]. The gel casting method was first used in the metals and ceramics processing group at Oak Ridge National Laboratory during the 1990s [15]. This relatively simple method was performed to solve challenges such as limitations in the production of parts with desired shape and size. This method can be used for the production of a wide range of materials including metals, ceramics, alloys and composites [16].

In recent years, the use of gel casting method for the production of various composites as well as porous products has been considered during various researches such as production of porous alumina composites containing nickel nanoparticles with nickel nitrate as a source of nickel and hydrogen gas as the reducing agent [5], porous alumina-nickel composite as a catalyst with nickel oxide as a source of supply of nickel and CO gas as a reducing agent [17], porous silicon carbide with carbon in resin as reducing agent and source of carbon and SiO as source of Si [17], alumina composite containing tungsten nanoparticles by gel casting method and tungsten in situ reduction [19], alumina-nickel composite with complex shapes by gel casting and using 3D printer technology [20], alumina-nickel composite by gel casting method and centrifugal method for fabrication of parts with high density and homogeneous properties [21], alumina-nickel layer composites by casting alumina gel between tungsten metal plates [22], making transparent alumina plates by gel casting with pressure control [23]. The study of the effect of thermal regime and atmosphere on the properties of alumina-nickel composite made of nickel powder by sol method was investigated by Zygmuntowicz et al. [24]. In addition, magnesium aluminate spinel with alumina and magnesium oxide by gel casting method [25], use of pre-sinter to improve the mechanical properties of alumina based composites made by gel casting [26], and recently, making high porosity alumina with suitable strength by gel casting method and optimizing the production process were invesitgated [27].

In this research, a porous alumina-nickel composite containing nickel nanoparticles was prepared by gel casting, in which for the first time, instead of using reducing gas, graphite particles (dispersed in the preformed body) were used as the reducing agent. The advantages of this new method are the reduction of nickel oxide by graphite instead of reducing gas removes the complex equipment from the system, the possibility of using conventional furnaces, the possibility of the composite production under air atmosphere, and creating the porosity in the composite body during the reduction process. All these advantages reduce production costs, in addition to the fact that the properties of the produced composite in terms of quality are quite competitive with the quality of the produced composite with other methods. Moreover, in this study, mechanical activation of the raw materials was used to control and change the temperature of the reduction process. Reduction with graphite compared to reduction with CO gas has the advantage such as uniform distribution of graphite particles in the composite and then removing graphite during the reduction process resulted in uniform distribution of porosity in the composite structure. Also, since graphite is an industrial lubricant and its coefficient of friction is low, so its presence in the gel casting process increases the slurry fluidity and more uniform filling of the mold and thus helps to improve the gel casting process.

2. MATERIALS AND METHODS

2. 1. Raw Materials   Raw materials, including nickel oxide, alumina, and graphite were used so that the final composite (after reduction and sintering) contained 5% V of nickel metal. The raw materials specifications used to prepare the slurry required for the gel casting process are given in Table 1.

In this research, two different methods namely Methods 1 and 2 were used to prepare the main samples of porous alumina-nickel composite and the resulting samples were named SM1 and SM2, respectively (Table 2). Also, various experiments using a mixture of the raw material without gel casting and only to investigate the NiO carbothermic reduction mechanisms were conducted according to the conditions given in Table 3.

TABLE 1. Specifications of the raw materials

Material	Purity (wt %)	Particle size (µm)	
α-Alumina	98.5	88	Iran Alumina
Nickel Oxide	99.9	2	Merck
Graphite	99	100 nm	Armina
Gelatin	98	<800	Microteb
CMC adhesive Carboxylmethyl callouses	99.5	<150	Yolung-china
Dispersant Tripolyphosphate sodium	99.8	<150	LYG-china

2. 2. Methods of Preparation and Characterization of Porous Alumina-nickel Composite The following methods were used to prepare the porous alumina-nickel composite:

Method 1: alumina powder mixed with 15 wt % ethanol and ball milled (20 minutes, rotation speed of 230 rpm, ball to powder ratio of 12) in a planetary ball mill (M200-Retsch-Germany) equipped with a polyethylene chamber and alumina balls. Next, the milled alumina was passed through a sieve (mesh 70 equivalents to 210 µm) and dried in an oven at 110 °C for 1 h. Graphite powder and nickel oxide were weighed based on reaction 1 (section 3.3) and their purity (Table 1). Then, they were ball milled in the air for 6 h with a ball to powder weight ratio of 12, at a rotation speed of 230 rpm.

To mix graphite powder and nickel oxide with alumina powder, these powders were milled for 5 minutes with the ball to powder weight ratio of 12 in air. In a solution containing 6 wt % gelatin, the gelatin powder was dissolved in distilled water for 2 hours at 45 °C with using a heater/magnetic stirrer [28]. The amount of distilled water required to prepare the gel casting slurry was subtracted from the amount of water in which the gelatin was dissolved. For the preparation of the gel casting slurry, the gelatin solution was mixed with graphite powder, nickel oxide, alumina, and distilled water, along with sodium triphosphate as a dispersant and CMC adhesive with specified weight ratios according to Table 2 using a mixer (model MY2011-NabBei) for 10 minutes. Then, the prepared slurry was poured into a cylindrical aluminum mold with a diameter of 1.5 cm and filled to a height of 1.5 cm. To dry the piece more evenly and prevent distortion and cracking, the mold was covered with a plastic bag and placed in an environment at a temperature of 20 °C for 72 h [29]. Then, the dried piece was removed from the mold.

Reduction and sintering processes were conducted in an electric furnace (Nobertherm-Ht 40/17) in the air. To prevent the oxidation of the reduced nickel, the piece was placed in an alumina crucible filled with carbon powder [30]. Then, the process was started from ambient temperature with a heating rate of 10 °C/min and continued until the furnace temperature reached 1200 °C. The piece was kept at 1200 °C for half an hour. Then, the process was continued with a heating rate of 2.5 °C/min to 1500 °C and it was kept at this temperature for half an hour. After finishing the process, the piece was gradually cooled in the furnace to room temperature.

Method 2: The difference between the first and second methods was in the ball milling time of alumina, nickel oxide, and graphite. To reduce the particle size of alumina and have a dense piece, the ball milling time of alumina in this method was 12 h at a speed of 230 rpm and the ball to powder weight ratio of 12. The ball-milling time of graphite and nickel oxide was 10 minutes just to increase their contact.

The phase analysis of the SM1 and SM2 samples was performed by XRD (X'pert PW 3040/60-Philips) at 25 °C with a step of 0.2 degrees using Cu-kα radiation. SEM images were prepared by Scanning Electron Microscope (VP 14500-LEO) and used to observe the

TABLE 2. Coding and preparation conditions of alumina-nickel composites

Code	Composition (wt %)							Ball milling time of graphite and nickel oxide mixture	Ball milling time of alumina ball milling	Sintering
	Alumina	Graphite	Nickel oxide	Gelatin	Dispersant	Distilled water	CMC adhesive			
SM1								6 h	20 min	Half an hour at a temperature of 1200 °C then increase the temperature to 1500 °C
SM2	58.63	1.36	8.50	0.75	2.50	28.2	0.075	10 min	12 h	

Other details were described in 2-2 section.

TABLE 3. Specifications of powder samples and conditions for TG-DTA tests

Code	Powder composition (wt %)			Ball milling time (min)	Ball to powder weight ratio	Rotation speed (rpm)	Atmosphere	Heating rate (°C/min)	TG-DTA model
	Nickel oxide	Graphite	Alumina						
A	86	14	0	10	12	230	Ar	10	Q600-TA
B	86	14	0	360	12	230	Ar	10	Q600-TA
C	12.8	2.10	85	720	12	230	Ar	10	Q600-TA

dimensions of the porosity and the presence of nickel particles in the alumina body. The density of prepared composites was measured using the immersion method (Archimedes method). The porosity percentage was then calculated according to the measured density and composite body dimensions. The optimal amount of the dispersant to have a slurry with the desired fluidity was determined by a rotary viscometer (Anton Paar –physical mcr 301).

2. 3. Nickel Oxide Reduction Mechanism   To investigate the reduction mechanism of carbothermic reduction of nickel oxide and to analyze the reactions that occur during heating of the SM1 and SM2 samples, the powder samples (containing graphite, nickel oxide, and alumina) without gel casting were prepared following the conditions given in Table 3 and analyzed by TG-DTA.

3. RESULTS AND DISCUSSIONS

3. 1. Characterization of Composite
3. 1. 1. Slurry Rheology and Dispersant Amount
The graph of viscosity changes in Figure 1 shows that with an increase in the amount of dispersant in the slurry containing 50 V% of the solid, the viscosity first decreases until the viscosity reaches a minimum value in the slurry containing 2.5 wt % dispersant. Figure 1 displays that increasing the dispersant amount excess than 2.5 wt %, slightly increases the slurry viscosity. The reason for this increase is that in the slurry containing 3.20 wt % of the dispersant, the slurry particles are saturated with the dispersant and the free ions in the slurry increased with viscosity [31]. It is observed that the viscosity curve of 1.8 % TPP in the range of 40-110 1/s is lower than the viscosity curve of 2.5 % TPP. That is related to the measurement error of the viscometer. Therefore, the 2.5 wt % dispersant is an optimum amount for the preparation of gel casting slurry.

3. 1. 2. Phase Analysis   The XRD patterns of SM1 and SM2 samples after the sintering process are shown in Figure 2. The XRD patterns show the alumina (α-alumina), metallic nickel, and nickel aluminate spinel are present in the composites. As can be seen in the XRD pattern of SM1, the metallic nickel main peak (45 degrees) is more intense than it in the XRD pattern of SM2. It confirms that mechanical activation of the nickel oxide and graphite mixture has improved the nickel oxide reduction (metallic nickel production) process. Nickel aluminate spinel is a blue to green pigment. The presence of this phase caused the color of the prepared composite to be green-blue. The formation of this phase has no negative effect on the properties of alumina-nickel composite. Nickel aluminate spinel has catalytic
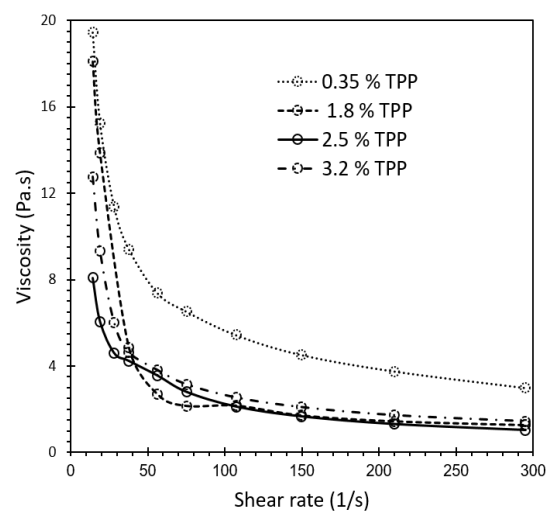

Figure 1. Rheological behavior of the gel casting slurry (50 V% of solid and 1 wt % of gelatin) containing the various amounts of dispersant

properties and is used in methane production process from hydrogen [32]. It has been suggested that the formation of nickel aluminate spinel in alumina-nickel catalysts increases the catalyst life [17].
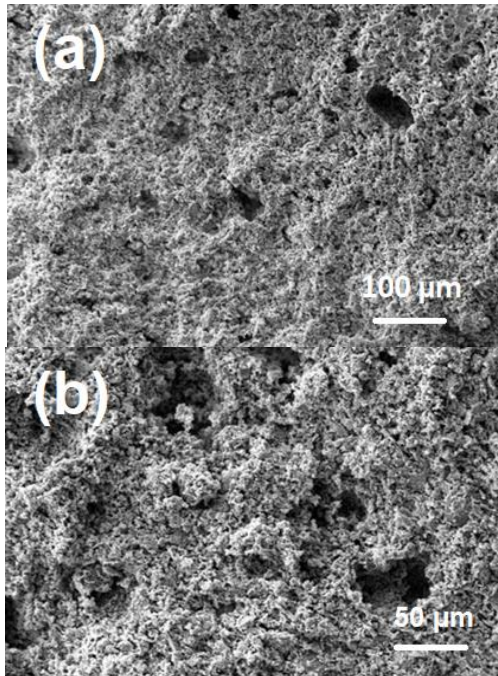
3. 2. Composite Microstructure   The SEM images in Figure 3 show the porosities in the structure of the SM2 sample. In these images, porosities with dimensions up to 50 microns can be observed. The results showed that the SM1 sample, in which alumina was milled for a shorter time, had more porosity than the SM2 sample. The porosities of SM1 and SM2 samples were 64 and 48% by volume, respectively. The longer milling time in the SM2 sample reduced the particle size and thus reduced the porosity in the sample.
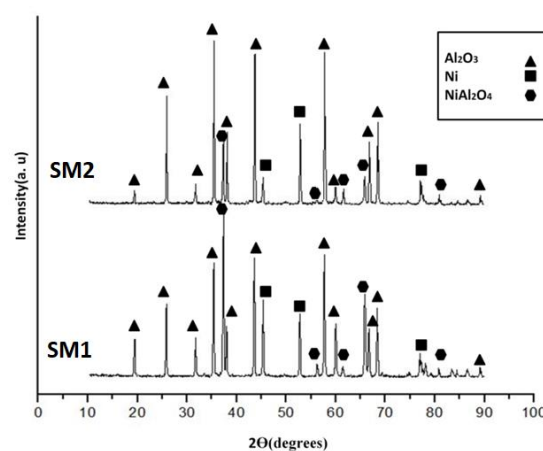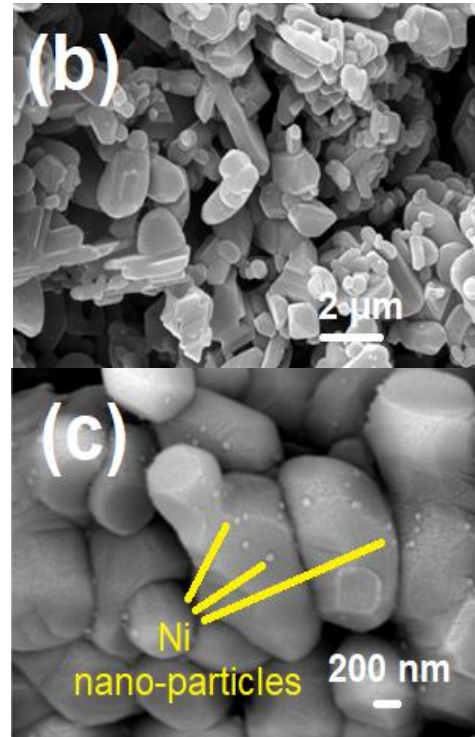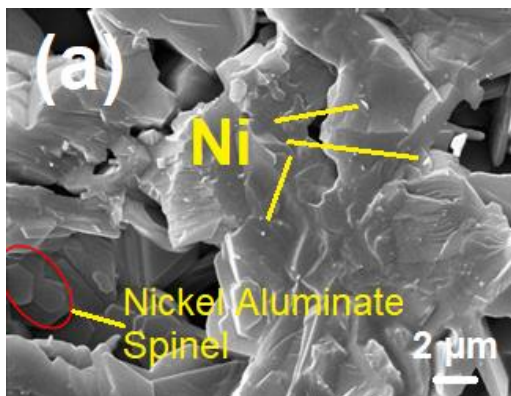

Figure 2. The XRD Pattern of SM1 and SM2 samples after the sintering process

Figure 4 shows the SEM images of the SM2 sample at a higher magnification. According to these images, the presence of nickel particles and a small amount of nickel aluminate spinel in the alumina field are quite clear. In Figure 4a, part of the alumina body is shown as a continuous phase, which indicates the proper connection and sintering of alumina after the sintering process. Nickel particles are seen in a light color. Figure 4b refers to the part of the composite that is deeper point from the surface. Figure 4c shows the nickel particles in nanometer dimensions. Alumina-nickel composites containing nickel nanoparticles have desired magnetic, optical, mechanical, and catalytic properties [5, 10]. Therefore, nickel nano-particles production by the method used in this research is a great advantage.


Figure 4. a) Structure of alumina-nickel composite-SM2, b) Structure of alumina-nickel composite-SM2 in the deeper point from the surface, c) Structure of alumina-nickel composite-SM2 containing Ni nano-particles

3. 3. Mechanism of Carbothermic Reduction of Nickel Oxide   The TG-DTA analyses of sample A are shown in Figure 5. It is seen that weight loss starts at 100 °C, which is related to the release of water absorbed by the powder. The weight loss continues up to 400 °C, which is related to the complete removal of bond water and volatiles. From 400 to 500 °C the weight is constant and no reaction occurs.

Figure 3. Porosities created in alumina-nickel composite (SM2) made by gel casting and reduction with graphite powder
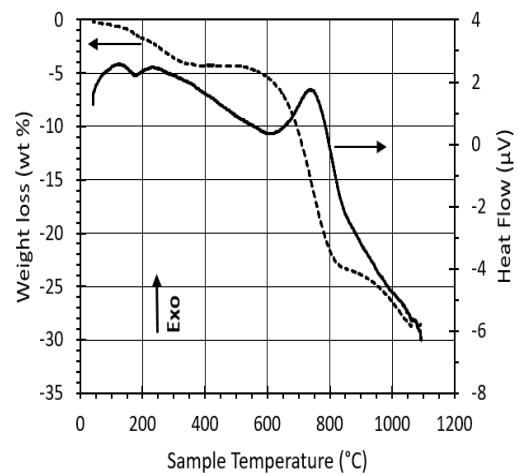
Figure 5. The TG-DTA curves of sample A

The reduction mechanism of most metal oxides with carbon, when there is no transition phase between the two materials, is described in two steps. In the first step (reaction 1), which is a slower step, the surface of the nickel oxide particles reacts with solid carbon. In the second step (reaction 2), the remained nickel oxide particles react with the CO gas resulted from reaction 1 [33]. Weight loss begins again at 500 ° C, which corresponds to the beginning of the reduction process of nickel oxide with graphite (Figure 5).

$$NiO + C = Ni + CO_{(g)} \tag{1}$$

$$NiO + CO_{(g)} = Ni + CO_{2\ (g)} \tag{2}$$
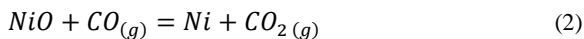
As can be seen in Figure 5, the rate of reaction 1 is initially slow. The diffusion of solid into solid (graphite and nickel oxide) is still low. As the temperature raised to 630 °C the reaction rate increased. Other studies have reported that the reaction of solid carbon with nickel oxide accelerated at high temperature close to 630 °C [34].

The solid-solid reaction takes place up to about 810 °C, and the slope continues to increase up to 810 °C. Here the second phase of the reaction, i.e. the reduction of nickel oxide with CO, begins and the rate of the reduction is reduced. There are two possible reasons for this decline. The first reason is that this temperature is the same as the temperature of CO formation; various studies have concluded that although CO itself is a reducing agent of nickel oxide, its formation initially slows down the reduction of nickel oxide with solid carbon. It is not clear why the presence of CO formation is an obstacle to the reduction reaction [33-35]. The formation of CO may consume some of the system energy and thus slow down the nickel oxide reduction process. The second reason is that at the beginning of CO formation, i.e. at a temperature of about 810 °C, the CO pressure has not yet reached a level that supports to react effectively. As a result, the reduction reaction as a whole was slowed down [33].

The TG-DTA analyses of sample B in Figure 6 show that due to the longer mechanical activation of sample B than sample A, the reduction reaction is initiated at a lower temperature (390 °C) than sample A (630 °C). According to Figure 6, in sample B, the onset temperature (775 °C) of the reaction rate decline is also lower than it in sample A (810 °C). It can be said that due to the reduction of nickel at a lower temperature and due to the catalytic role of nickel, the beginning of the carbon monoxide formation has also started from a lower temperature [35].

According to TG curves in Figures 5 and 6, the overall weight losses at 800 °C for samples A and D are 22 and 29 wt %, respectively. The loss of weight is equivalent to oxygen removal of the specimens during

NiO reduction. This confirms that the mechanical activation not only decreases the reduction temperature but also increases the metallic nickel production.

To investigate the effect of alumina in the reduction process, a thermal analysis was performed for the sample containing alumina (sample C) (Figure 7). A comparison of Figures 7 and 5 shows that the presence of alumina does not affect the reduction process. In general, the peaks in Figure 5 (sample A) are clearer than in Figure 7 (sample C) because sample A contains only graphite and nickel oxide. The slope of Figure 7 is due to the high thermal resistance of alumina resulted in a high heating rate during thermal analysis [36].
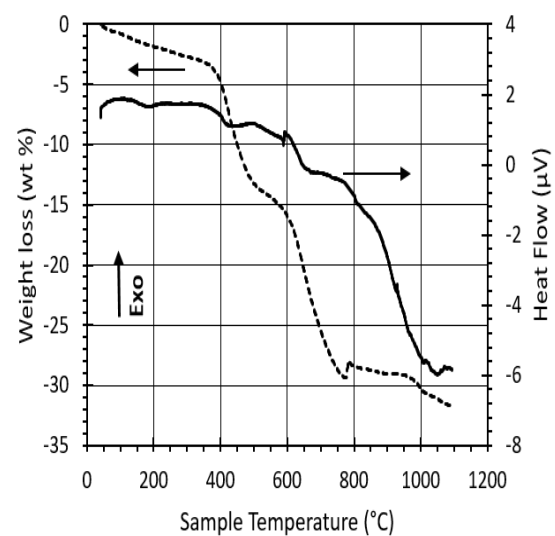

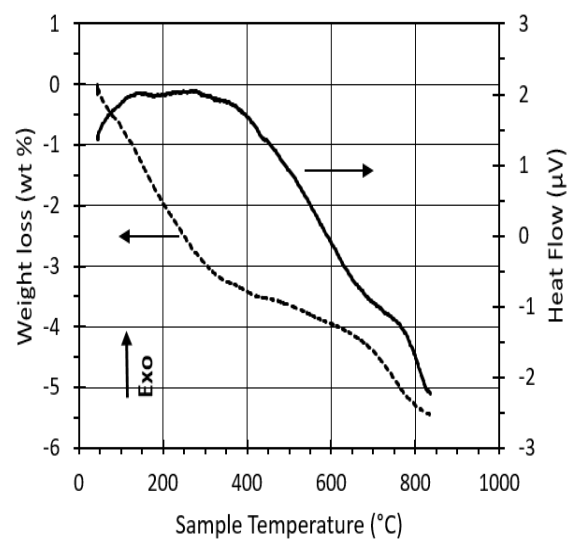**Figure 6.** The TG-DTA curves of sample B

Figure 7. TG-DTA curves of sample C

4. CONCLUSION

The following conclusions were obtained from this research:
1. The optimum amount of tripolyphosphate sodium as a dispersant for preparation of a slurry with 50 V% of solid (alumina, graphite, and nickel oxide) was 2.5 wt %.
2. The porosity of the sample made with 12 h ball-milled alumina was 48% and it was 64 % in the sample made with 20 min ball-milled alumina.
3. The presence of nickel seems to reduce the temperature of CO formation during the Boudouard reaction due to its catalytic effect.
4. Due to the mechanical activation of the graphite and nickel oxide mixture for 6 h, more nickel was reduced than the inactivated sample.
5. In addition to alumina and nickel nano-particles, the sample also contained nickel aluminate spinel.
6. The mechanical activation of raw materials decreased the NiO reduction temperature and increased the metallic Ni production.

5. REFERENCES

1. Saindane, U. V., Soni, S., Menghani, J. V. "Dry Sliding Behavior of Carbon-Based Brake Pad Materials." *International Journal of Engineering, Transactions B: Applications*, Vol. 34, No. 11, (2021), 2517-2524. DOI: 10.5829/ije.2021.34.11b.14

2. Saindane, U. V., Soni, S., Menghani, J. V. "Studies on Mechanical Properties of Brake Friction Materials Derived from Carbon Fibres Reinforced Polymer Composite." *Materials Today: Proceedings*, Vol. 47, No. 17, (2021), 5760-5765. DOI: 10.1016/j.matpr.2021.04.079

3. Dehaghani, M. T., Ahmadian, M. "Fracture Mechanism of CoCrMo Porous Nano-Composite Prepared by Powder Metallurgy Route." *International Journal of Engineering, Transactions A: Basics*, Vol. 31, No. 1, (2018), 19-24. DOI: 10.5829/ije.2018.31.01a.03

4. Nekokar, N., Pourabdoli, M. "Isothermal Redox Kinetics of Co_3O_4-Fe_2O_3 Nano-Composite as a Thermochemical Heat Storage Material.", *International Journal of Engineering, Transactions B: Applications*, Vol. 32, No. 8, (2019), 1200-1209. DOI: 10.5829/ije.2019.32.08b.17

5. Niihara, K., Kim, B. S., Nakayama, T., Kusunose, T., Nomoto, T., Hikasa, A., Sekino, T. "Fabrication of Complex-Shaped Alumina/Nickel Nanocomposites by Gel Casting Process." *Journal of the European Ceramic Society*, Vol. 24, No. 12, (2004), 3419-3425. https://doi.org/10.1016/j.jeurceramsoc.2003.10.027

6. Kim, B. S., Sekino, T. , Nakayama, T. , Kusunose, T., J. S. Lee, K. Niihara. "Mechanical and Magnetic Properties of Alumina/Nickel Nano Composites Prepared by Pulse Electric Current Sintering." *Journal of Ceramic Society of Japan*, Vol. 111, No. 1295, (2003), 257-460.

7. Kritikaki, A., Tsetsekou, A. "Fabrication of Porous Alumina Ceramics from Powder Mixtures with Sol–Gel Derived Nanometer Alumina: Effect of Mixing Method." *Journal of the European Ceramic Society*, Vol. 29, (2009),1603-1611. DOI: 10.1016/j.jeurceramsoc.2008.10.011

8. Sekino, T., Nakajima, T., Ueda, S., Niihara, K. "Reduction and Sintering of a Nickel-Dispersed-Alumina Composite and its

9. Properties" *Journal of the American Ceramic Society*, Vol. 8, (1997), 1139-1148. https://doi.org/10.1111/j.1151-2916.1997.tb02956.x

10. Sekino, T., Nakajima, T., Niihara, K. "Mechanical and Magnetic Properties of Nickel Dispersed Alumina-Based Nanocomposite." *Materials Letters*, Vol. 29, (1996), 165-169. https://doi.org/10.1016/S0167-577X(96)00136-X

11. Roy, B., Martinez, U., Loganathan, K., Datye, A. K., Leclerc, C.A. "Effect of Preparation Methods on the Performance of Ni/Al_2O_3 Catalysts for Aqueous-Phase Reforming of Ethanol: Part I-Catalytic Activity." *International Journal of Hydrogen Energy*, Vol. 37, (2012), 8143-8153. https://doi.org/10.1016/j.ijhydene.2012.02.056

12. Zhao, A., Ying, W., Zhang, H., Ma, H., Fang, D. "Ni-Al_2O_3 Catalysts Prepared by Solution Combustion Method for Syngas Methanation." *Catalysis Communications*, Vol. 17, (2012), 34-38. https://doi.org/10.1016/j.catcom.2011.10.010

13. Koclar, G. S. "Gelcasting of Alumina Ceramics with Gelatin and Carrageenan Gum and Investigation of Their Mechanical Properties." M.Sc. Thesis, Materials science and engineering, Izmir Institute of Technology, 2013.

14. Dhara, S., Kamboj, R. K., Pradhan, M., Bhargava, P. "Shape Forming of Ceramics via Gel Casting of Aqueous Particulate Slurries." *Journal of Bulletin of Materials Science*, Vol. 6, (2002), 565-568. DOI: 10.1007/BF02710552

15. Pabst, W. , Gregorová, E. , Havrda, J. , Týanová, E. Gelatin casting and starch consolidation of alumina ceramics", Book chapter in Ceramic Materials and Components for Engine*s*, WILEY-VCH Verlag GmbH, 2001, pp. 587-592.

16. Omatete, O. O., Janney, M. A., Nunn, S. D. "Gel Casting: From Laboratory Development to Industrial Production." *Journal of the European Ceramic Society*, Vol. 17, (1997), 407– 413. https://doi.org/10.1016/S0955-2219(96)00147-1

17. Tari, G. "Gel Casting Ceramics: A Review." *American Ceramic Society Bulletin*, Vol. 82, No. 4, 43-46.

18. Becerra, A. M., Castro-Luna, A. E. "An Investigation on the Presence of $NiAl_2O_4$ in a Stable Ni on Alumina Catalyst for Dry Reforming." *Journal of the Chilean Chemical Society*, Vol. 2, (2005), 465-469. http://dx.doi.org/10.4067/S0717-97072005000200005

19. Cheng, H., Yang, J. F., Zhang, N. L. "Fabrication and Characterization of Hierarchical Porous SiC Ceramics via Gel Casting and Carbothermal Reduction Between Carbon and SiO." *Journal of the Ceramic Society of Japan*, Vol. 128, No. 9, (2020), 589-594. DOI: DOI:10.2109/jcersj2.20063

20. Zygmuntowicz, J., Piątek, M., Miazga, A., Konopka, K., Kaszuwara W. "Dilatrometric sintering study and Characterization of Alumina-Nickel Composites." *Processing and Application of Ceramics*, Vol. 12, No. 2, (2018), 111-117. DOI:10.2298/PAC1802111Z

21. Ndinisa, S. S., Whitefield, D. J., Sigalas, I. "Fabrication of Complex Shaped Alumina Parts by Gel Casting on 3D Printed Moulds." *Ceramics International*, Vol 46, No. 3, (2020), 3177-3182. https://doi.org/10.1016/j.ceramint.2019.10.021

22. Zygmuntowicz, J., Zielant, D., Suchecki, P., Konopka, K., Kaszuwara, W. "Fabrication of Al_2O_3-Ni Graded Composites by Centrifugal Casting in an Ultracentrifuge.", *Composites Theory and Practice*, Vol. 18, No. 3, 174-179.

23. Kedzierska-Sar, A., Starzonek, S., Kukielski, M., Falkowski, P., Rzoska, S. J., Szafran, M. "Gelcasting of Al_2O_3–W Composites: Broadband Dielectric Spectroscopy and Rheological Studies of Tungsten Influence on Polymerisation Kinetics, *Ceramics International*, Vol. 45, No. 12, 15237-15243. https://doi.org/10.1016/j.ceramint.2019.05.012

24. Chen, H., Shunzo, S., Zhao, J., Di, Z. "Pressure Filtration Assisted Gel Casting in Translucent Alumina Ceramics

Fabrication.", *Ceramics International*, Vol 44, No. 14, 16572-16576. DOI: 10.1016/j.ceramint.2018.06.079

24. Zygmuntowicz, J., Wiecinska, P., Miazga, A., Konopka, K., Szafran, M., Kaszuwara, W. "Thermoanalytical Studies of the Ceramic-Metal Composites Obtained by Gel-Centrifugal Casting." *Journal of Thermal Analysis and Calorimetry*, Vol. 133, No. 1, (2018), 303-312. https://doi.org/10.1007/s10973-017-6647-z

25. Shahbazi, H., Shokrollahi, H., Tataei, M. "Gel-Casting of Transparent Magnesium Aluminate Spinel Ceramics Fabricated by Spark Plasma Sintering (SPS)." *Ceramics International*, Vol. 44, No. 5, (2018), 4955-4960. DOI: 10.1016/j.ceramint.2017.12.088

26. Lv, L., Lu, Y., Zhang, X., Chen, Y., Hou, W., Liu, W., Yang, J. "Preparation of Low-Shrinkage and High-Performance Alumina Ceramics via Incorporation of Pre-Sintered Alumina Powder Based on Isobam Gelcasting." *Ceramics International*, Vol 45, No. 9, 11654-11659. https://doi.org/10.1016/j.ceramint.2019.03.039

27. Zhang, M. et al. "High-Strength Macro-Porous Alumina Ceramics with Regularly Arranged Pores Produced by Gel-Casting and Sacrificial Template Methods." *Journal of Materials Science*, Vol. 54, No. 14, (2019), 10119-10129. https://doi.org/10.1007/s10853-019-03576-8

28. Montanaro, L., Coppola, B., Palmero, P., Tulliani, J. M. "A Review on Aqueous Gel Casting: A Versatile and Low-Toxic Technique to Shape Ceramics." *Ceramics International*, Vol. 45, No. 7, (2019), 9653-9673. DOI: 10.1016/j.ceramint.2018.12.079

29. Esfahani, H. B., Yekta, B. E., Marghussian, V. K. "Rheology and Gelation Behavior of Gel-Cast Cordierite-Based Glass Suspensions." *Ceramic International*, Vol. 38, (2011),1175-1179. DOI: 10.1016/j.ceramint.2011.08.046

30. Chan, C. F. , Argent, B. B. , Lee, W. E. "Influence of Additives on Slag Resistance of Al_2O_3-SiO_2-SiC-C Refractory Bond Phases Under Reducing Atmosphere." *Journal of the American Ceramic Society*, Vol. 81, (1998), 3177-3188. https://doi.org/10.1111/j.1151-2916.1998.tb02754.x

31. Kim, H. M., Venkatesh, R. P., Kwon, T. Y., Park, J. G. "Influence of Anionic Polyelectrolyte Addition on Ceria Dispersion Behavior for Quartz Chemical Mechanical Polishing." *Colloids and Surfaces A: Physicochemical and Engineering Aspects*, Vol. 411, (2012), 122-128. https://doi.org/10.1016/j.colsurfa.2012.07.009

32. Ding, C., Liu, W., Wang, J., Liu, P., Zhang, K., Gao, X., Ding, G., Liu, S., Han, Y., Mac, X. "One Step Synthesis of Mesoporous NiO–Al_2O_3 Catalyst for Partial Oxidation of Methane to Syngas: The Role of Calcination Temperature." *Fuel*, Vol. 162, (2015), 148-154. https://doi.org/10.1016/j.fuel.2015.09.002

33. Lebukhova, N. V., Karpovich, N. F. "Carbothermic Reduction of Copper, Nickel, and Cobalt Oxides and Molybdates." *Inorganic Materials*, Vol. 8 (2008), 1003-1007. DOI: https://doi.org/10.1134/S0020168508080207

34. L'vov, B. V. "Mechanism of Carbothermal Reduction of Iron, Cobalt, Nickel and Copper Oxides." *Thermochimica Acta*, Vol. 360, No. 2, (2000), 109-120. DOI: 10.1016/S0040-6031(00)00540-2

35. Yang, H., McCormic, P.G. "Mechanically Activated Reduction of Nickel Oxide." *Metallurgical and Materials Transactions B*, Vol. 29, (1998), 29, 449-455. https://doi.org/10.1007/s11663-998-0123-x

36. Haines, P. J., Principles of thermal analysis and calorimetry, The Royal Society of Chemistry, Cambridge, 2002.

Persian Abstract

چکیده

اثر میزان پراکنده ساز (تری پلی فسفات سدیم) بر ویسکوزیته ژل و فعال سازی مکانیکی مواد اولیه، ترکیب مخلوط مواد اولیه و اتمسفر احیا روی کامپوزیت های تهیه شده و مکانیسم احیا NiO مورد بررسی قرار گرفت. مشخص شد که 2/5 درصد وزنی پراکنده ساز برای یک سوسپانسیون ژل با 50 درصد حجمی جامد متشکل از آلومینا، گرافیت و اکسید نیکل مقدار بهینه ای است. نتایج XRD محصول احیا و سینتر شده (در دمای 1500–1200 درجه سانتیگراد) نشان داد که اسپینل آلومینا، نیکل و آلومینات نیکل در کامپوزیت تهیه شده وجود دارد. تخلخل کامپوزیت ساخته شده با آلومینای آسیاشده به مدت 4 ساعت، 48 درصد و تخلخل کامپوزیت تهیه شده با آلومینای آسیاشده به مدت 20 دقیقه، 64 درصد بود. نتایج TG-DTA نشان داد که دما و مکانیسم احیا به زمان آسیاکاری مواد اولیه بستگی دارد. آنالیز حرارتی نشان داد که فعال سازی مکانیکی مواد اولیه باعث کاهش دمای احیا NiO و افزایش تولید نیکل فلزی می شود.